doi:10.1038/nature24057

Supplementary Information

Table of Content

Supplementary Note 1: Arterial and venous circulating metabolite labeling and turnover flux

Glucose production rate is typically determined using main text Eqn. [2], based on labeled glucose infusion and measurement of venous glucose labeling. Eqn. [2] was derived based on the assumption that the circulatory system approximates a single well-mixed liquid pool. For lactate, arterial and venous labeling diverge, and this divergence has resulted in substantial debate in the literature about the biological meaning of lactate labeling data (see main text for relevant citations). Here we re-examine the basic assumptions underlying Eqn. [2], with a particular focus on the causes and consequences of arterial-venous labeling differences. Through both partial differential equation modeling of labeling gradients across a single tissue and a more generalized model that includes any numbers of tissues, we establish the general validity of Eqn. [2] with turnover flux measured based on arterial labeling data. We also establish the quantitative relationship between arterial-venous labeling differences and turnover flux, as shown in main text Eqn. [3].

1. Model of single well-mixed pool

In the absence of tracer, at metabolic steady state, the rate at which tissues collectively consume a metabolite from the arterial circulation ($F_{consumption}$) and excrete the metabolite into the venous circulation ($F_{production}$) are equal and define the metabolite's circulatory turnover flux (F_{circ}). Previous literature refers to $F_{production}$ and $F_{consumption}$ as rate of appearance R_a and rate of disappearance R_d, respectively[1]. While the choice of symbols does not affect the downstream analysis, we prefer the term circulatory turnover flux to emphasize that F_{circ} is flux and that influx and efflux from the circulation balance.

Consider first the simple case where metabolite turnover is slow relative to circulatory carrying capacity ($F_{circ} \ll Q \cdot C$) and thus the whole circulatory system resembles a single well mixed liquid pool. This is the situation which has been assumed in prior literature that attempts to quantitatively measure F_{circ}. As shown in Fig. S1, metabolite production released from tissues ($F_{production}$) and tracer infusion (R) feed into a common circulatory pool which is drained by tissue metabolite consumption ($F_{consumption}$). The amount of the labeled form in the pool is denoted as M^L and the amount of the unlabeled form as M^U. The fraction of the labeled form in the pool is measured as labeling enrichment $L = \frac{M^L}{M^U+M^L}$. Here M^L refers specifically to circulating metabolite in the same labeling state as the infused tracer. For example, if the tracer is U-^{13}C-glucose, then partially labeled glucose is counted as unlabeled, as it comes from endogenous glucose production, not from tracer infusion.

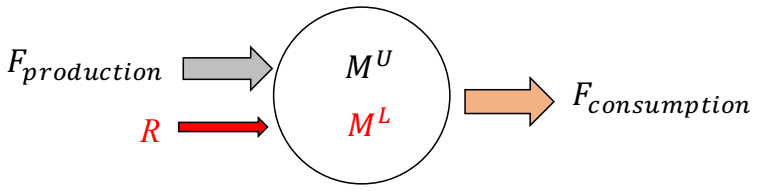

Figure S1. A model of infusing into a single well-mixed pool.

The change of the amount of the labeled form follows the simple kinetic equation,

$$\frac{dM^L}{dt} = R - L \cdot F_{consumption} \quad [S1.1]$$

where for the last term we have used the assumption that the pool is well mixed (so that the outgoing flux for the labeled form is proportional to the fraction of the labeled form in the total pool).

At steady state, metabolite labeling is given by

$$L = \frac{R}{F_{consumption}} \quad [S1.2]$$

Note also at steady state that

$$F_{consumption} = R + F_{production} \quad [S1.3]$$

We thus have

$$L = \frac{R}{F_{production}+R} \quad [S1.4]$$

Assuming that tracer infusion is accommodated by increased $F_{consumption}$ without changing $F_{production}$, and hence define

$$F_{circ} = F_{production} \quad [S1.5]$$

Combining Eqns. [2.4] and [2.5], we have

$$F_{circ} = \frac{R(1-L)}{L} \quad [S1.6]$$

which is shown as Eqn. [2] in the main text.

Note that the impact of labeled metabolite infusion on endogenous flux depends on the physiological regulatory mechanisms involved. Consistent with the glucose production rate literature[2-4], here we assume that the $F_{production}$ is not altered and that the infused labeled metabolite is absorbed by increased $F_{consumption}$. This need not be the case. For example, if an ultrasensitive negative feedback regulatory mechanism maintains a nearly constant metabolite pool, $F_{production}$ may decrease rather than $F_{consumption}$ increasing. In such cases, $F_{circ} = F_{consumption} = \frac{R}{L}$, which differs from Eqn. [S1.6] by the term $1 - L$. Therefore, Eqn. [S1.6] is subject to systematic relative error of magnitude L. For this reason, low labeling ($L \ll 1$) favors accurate measurement of F_{circ}. On the flipside, higher labeling ($L \gg 0$) facilitates more precise measurement of L. To balance these factors, we selected infusion rates to achieve $L \approx 10\%$.

2. *A partial differential equation model that accounts for arterial-venous tracer enrichment differences*

A complication in prior reported measurements of the lactate turnover flux involved differences in arterial and venous lactate labeling[5-11]. Because we infuse into the right atrium and labeled metabolite is cleared by the tissues, arterial labeling always exceeds venous labeling. The question is the magnitude and significance of the difference. Conceptually, the enrichment difference depends both on the metabolite's tissue transformation rate and on its physical flow through the tissue carried by the blood stream. When the metabolite's circulatory flow (cardiac output Q × concentration C) is much greater than its tissue biochemical transformation rate (F_{circ}) then arterial-venous differences are minimal and the entire system acts as a single well-

mixed pool. Here we develop a more general model, based on partial differential equations, which works also when F_{circ} is similar to $Q \cdot C$.

Instead of treating a tissue as one well-mixed compartment, we introduce a position dependent enrichment of isotopic labeling $L(x)$ within a tissue along the dimension x from the arterial inflow to the venous outflow. As tissues are connected in parallel to the artery and the vein, for simplicity, here we consider only a single generic cylindrical tissue with cross sectional area of A and length of l (Fig. S2). Other parameters are defined in Fig. S2.

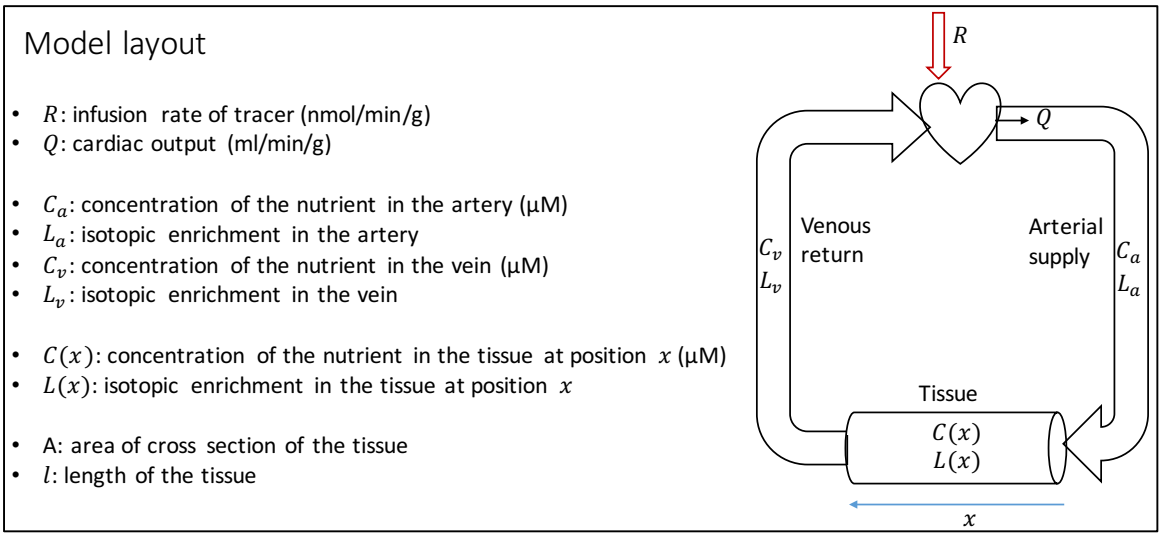

Figure S2. Layout of the partial differential equation model.

Defining the circulatory turnover flux

Similar to the definition of F_{circ} that leads to Eqn. [S1.5], here F_{circ} is defined as the production flux that is released by tissues into the systemic venous circulation. This definition distinguishes F_{circ} from the total production flux, as some of the production flux may be consumed by the tissue locally. To define F_{circ} mathematically, we first note that inside the tissue, the infused metabolite can be regarded as composed of three components, the labeled form $C^L(x)$, the newly produced component which is unlabeled $C^U_{new}(x)$, and the "old" unlabeled component which flows to the tissue from the artery $C^U_{old}(x)$, i.e.,

$$C(x) = C^L(x) + C^U_{new}(x) + C^U_{old}(x) \quad [S1.7]$$

The circulatory turnover flux is then defined by

$$F_{circ} = Q \cdot C^U_{new}(x = l) \quad [S1.8]$$

where $C^U_{new}(x = l)$ is the venous concentration of the newly produced metabolite. With this definition, in the following, we re-derive the expression for F_{circ} in terms of the infusion rate and circulating metabolite labeling.

Differential metabolite labeling across tissue

To model the change of each of the three metabolite components across a tissue, we consider a thin slice of tissue of cross section area A and of width Δx.

Labeled form: The amount of the labeled form of the metabolite within this tissue slice at time t is $C^L(x,t)\cdot A\cdot \Delta x$. The time dependence of the amount is then described by

$$\frac{d(C^L(x,t)\cdot A\cdot \Delta x)}{dt} = C^L(x,t)\cdot Q - C^L(x+\Delta x,t)\cdot Q - k\cdot C^L(x,t)\cdot A\cdot \Delta x \quad [S1.9]$$

where the first and second terms of the right hand side are the bloodstream-carried incoming and outgoing fluxes to and from the tissue slice, respectively, and the third term is the consumption flux of the tissue with k as the reaction constant. Rearranging Eqn. [S1.9] and taking the limit $\Delta x \to 0$, we obtain a partial differential equation describing the temporal and spatial dependences of isotopic labeling in the tissue,

$$\frac{dC^L(x,t)}{dt} = -\frac{dC^L(x,t)}{dx}\cdot\frac{Q}{A} - k\cdot C^L(x,t) \quad [S1.10]$$

At steady state, Eqn. [S1.10] becomes

$$\frac{dC^L(x)}{dx}\cdot\frac{Q}{A} + k\cdot C^L(x) = 0 \quad [S1.11]$$

And its solution is

$$C^L(x) = C_a^L\cdot e^{-\frac{k\cdot A}{Q}\cdot x} \quad [S1.12]$$

where $C^L(x=0) = C_a^L$ is the concentration of labeled form in the artery.
The concentration of the labeled form in the vein (C_v^L) is given by

$$C_v^L = C_a^L\cdot e^{-\frac{k\cdot A\cdot l}{Q}} \quad [S1.13]$$

Old unlabeled component: For the old unlabeled form of the metabolite, it follows similar kinetics as the labeled form and similar derivation yields

$$C_{old}^U(x) = C_a^U\cdot e^{-\frac{k\cdot A}{Q}\cdot x} \quad [S1.14]$$

where C_a^U is the unlabeled metabolite in the artery.

Newly made component: For the newly made metabolite, the change of its amount in the tissue slice follows

$$\frac{d(C_{new}^U(x,t)\cdot A\cdot \Delta x)}{dt} = C_{new}^U(x,t)\cdot Q - C_{new}^U(x+\Delta x,t)\cdot Q + j_P\cdot A\cdot \Delta x - k\cdot C_{new}^U(x,t)\cdot A\cdot \Delta x \quad [S1.15]$$

where j_P is the specific production rate of the metabolite (i.e., production rate per tissue volume). The PDE version of Eqn. [S1.15] is

$$\frac{dC_{new}^U(x,t)}{dt} = -\frac{dC_{new}^U(x,t)}{dx}\cdot\frac{Q}{A} + j_P - k\cdot C_{new}^U(x,t) \quad [S1.16]$$

And the ODE at steady state is

$$\frac{dC_{new}^U(x)}{dx}\cdot\frac{Q}{A} - j_P + k\cdot C_{new}^U(x) = 0 \quad [S1.17]$$

It solution is

$$C_{new}^U(x) = \frac{j_P}{k}\cdot\left(1 - e^{-\frac{k\cdot A}{Q}\cdot x}\right) \quad [S1.18]$$

which correctly produces that $C_{new}^U(x=0) = 0$.

Expression of the circulatory turnover flux

Using Eqn. [S1.18] and with the definition of F_{circ} in Eqn. [S1.8], we have the expression of F_{circ} as

$$F_{circ} = Q \cdot \frac{j_P}{k} \cdot (1 - e^{-\frac{k \cdot A \cdot l}{Q}}) \quad [S1.19]$$

Substituting Eqns. [S1.12], [S1.14], and [S1.18] into Eqn. [S1.7], we get

$$C(x) = C_a \cdot e^{-\frac{k \cdot A}{Q} \cdot x} + \frac{j_P}{k} \cdot (1 - e^{-\frac{k \cdot A}{Q} \cdot x}) \quad [S1.20]$$

Thus in the vein,

$$C_v = C(x = l) = C_a \cdot e^{-\frac{k \cdot A \cdot l}{Q}} + \frac{j_P}{k} \cdot (1 - e^{-\frac{k \cdot A \cdot l}{Q}}) \quad [S1.21]$$

Using Eqns. [S1.13] and [S1.21] to replace the tissue related parameters in Eqn. [S1.19], we obtain

$$F_{circ} = Q \cdot C_v \cdot \frac{L_a - L_v}{L_a} = Q \cdot C_v - \frac{Q \cdot C_v \cdot L_v}{L_a} \quad [S1.22]$$

Since mass balance of total amount and the labeled form of the metabolite in the artery requires that

$$R = Q \cdot (C_a - C_v) \quad [S1.23]$$

and

$$R = Q \cdot (C_a^L - C_v^L) = Q \cdot C_a \cdot L_a - Q \cdot C_v \cdot L_v \quad [S1.24]$$

Eqn. [S1.22] becomes

$$F_{circ} = \frac{R(1 - L_a)}{L_a} \quad [S1.25]$$

by substituting $Q \cdot C_v \cdot L_v$ from Eqn. [S1.24] into Eqn. [S1.22] and then using Eqn. [S1.23]. Thus, in cases where metabolite turnover is sufficiently fast to produce arterial-venous labeling differences, with use of arterial labeling data, Eqn. [2] of the main text still holds.

Note that an equation for calculating the cardiac output can be derived from Eqns. [S1.22] and [S1.25],

$$Q = \frac{R}{C_v} \cdot \frac{1 - L_a}{L_a - L_v}$$

where all the parameters are given or can be accurately measured.

Dependence of the turnover flux on tissue metabolic rate and blood flow rate

With Eqns. [S1.19] and [S1.21], the circulatory turnover flux can be expressed as

$$F_{circ} = Q \cdot C_v - Q \cdot C_a \cdot e^{-\frac{k \cdot A \cdot l}{Q}} \quad [S1.26]$$

With Eqn. [S1.23], it becomes

$$F_{circ} = Q \cdot C_a \cdot (1 - e^{-\frac{k \cdot A \cdot l}{Q}}) - R \quad [S1.27]$$

or

$$F_{circ} = Q \cdot C_a \cdot (1 - e^{-\frac{k}{q}}) - R \quad [S1.28]$$

where $q = \frac{Q}{A \cdot l}$ is the volumetric blood flow rate. [For mouse, $Q \approx 0.53\ ml/min/g$[12-16]. The tissue volume $A \cdot l \approx 1 ml/g$. Therefore, the volumetric blood flow rate in mouse is $q \approx 0.5/min$.]

This equation describes an asymptotic exponential approach of turnover flux towards the circulatory carrying capacity $Q \cdot C$ as the quantity $\frac{k}{q}$ which measures the relative magnitude between the tissue metabolic rate k and the volumetric blood flow rate q, increases. For relatively slow metabolic rate ($q \gg k$),

$$F_{circ} \approx k \cdot C_a \cdot A \cdot l - R \quad [S1.29]$$

or

$$F_{circ} \approx\cdot F_{consumption} - R \quad [S1.30]$$

which recovers what we have in the case of single well-mixed pool. For relatively fast metabolic rate ($q \ll k$),

$$F_{circ} \approx Q \cdot C_a - R \quad [S1.31]$$

meaning that F_{circ} nears the upper bound $Q \cdot C$, as stipulated in Eqn. [1] in the main text.

Arterial and venous enrichment differences and turnover flux

Rearranging Eqn. [S1.22] yields Eqn. [3] in the main text,

$$\frac{\Delta L}{L_a} = \frac{F_{circ}}{Q \cdot C_v} \quad [S1.32]$$

where $\Delta L = L_a - L_v$. In practice, since we infuse only trace amount of labeled metabolite, the infusion rate is much smaller than the turnover flux, $R \ll F_{circ} < Q \cdot C_a$, and subsequently $C_a \approx C_v$. We can therefore assume a constant metabolite concentration C throughout the system. Thus,

$$\frac{\Delta L}{L_a} \approx \frac{F_{circ}}{Q \cdot C} \quad [S1.33]$$

This equation relates the turnover flux to the relative difference between the arterial and venous labeling ($\frac{\Delta L}{L_a}$): the bigger the difference is, the closer the turnover flux is to its upper bound $Q \cdot C$. For lactate in the fasted state, $\frac{\Delta L}{L_a} \approx 0.3$, indicating that the turnover flux of lactate reaches about 30% of the maximal carrying capacity by the blood flow. Eqn. [S1.33] can also be used to calculate F_{circ} for lactate. Using $Q = 0.53 \pm 0.11$ ml/min/g[12-16] and $C = 2.5 \pm 0.2$ mM[17], together with $\frac{\Delta L}{L_a} \approx 0.3$, we get lactate F_{circ} as 398 ± 88 nmol/min/g in fasted state, which is comparable to the value of 374 ± 112 nmol/min/g obtained with Eqn. [2]. Eqn. [S1.33] was used to estimate arterial lactate labeling in the fed state, with the estimated arterial lactate enrichment used for all subsequent fed state calculations. For pyruvate, venous labeling following tracer infusion is low and implies a large arterial-venous labeling difference and accordingly we report pyruvate F_{circ} as $Q \cdot C$ in Table 1, using $C = 108.3 \pm 13.7$ μM[17].

Calculating the contribution of circulating metabolites to tissue metabolites

We define the normalized labeling $L_{B \leftarrow A}$ from an infused ^{13}C-labeled circulating metabolite A into a downstream tissue product B as,

$$L_{B \leftarrow A} = \frac{L_t^B}{L_a^A} \quad [S1.34]$$

where L_t^B is the fraction of ^{13}C-labeled carbon in B in the tissue and L_a^A is the fraction of ^{13}C-labeled carbon in A in the arterial circulation. This definition specifically captures the contribution of incoming circulating precursor (carried to the tissue by the arterial circulation) to the downstream metabolic product. It omits any contribution to the product coming from precursor which is made, released into the circulation, and reabsorbed within the tissue. In this respect, the definition is both conservative (i.e. leads to lower estimates of fractional lactate contributions to TCA intermediates) and properly reflects our interest in inter-organ metabolite exchange.

L_a^A and L_t^B (used in the calculation of $L_{B\leftarrow A}$) are defined as the average labeling on a per carbon atom basis of circulating A and tissue B. For example, let M_A be the mass isotopomer distribution (which is a vector representing the fractional abundance of different ^{13}C-labeled forms) of A

$$M_A = [A_0, A_1, A_2, \dots, A_n] \quad \text{[S1.35]}$$

where n is the number of carbon atoms in A.
Then

$$L_a^A = \frac{M_A \cdot N}{n} \quad \text{[S1.36]}$$

where N is the column vector of $[0, 1, 2, \dots, n]$.
Note that calculation of F_{circ} is not based on this average carbon labeling but rather only the fraction of the labeled infused form (such that any biochemical transformations which alter the labeling contribute equally to F_{circ}). Specifically, if A is infused in fully labeled form, then F_{circ} is calculated solely based on M_A's last element A_n irrespective of the abundances of the other labeled forms.

3. *A more generalized model including multiple tissues that accounts for arterial-venous tracer enrichment differences*

Consider multiple tissues connected to the circulation. Although Fig. S3 shows only two tissues i and j, the model applies to any number of tissues.

Tissue-specific production flux

Let us focus on one tissue first. As in Eqn. [S1.7], we have for tissue i,

$$C_i(x) = C_i^L(x) + C_{old,i}^U(x) + C_{new,i}^U(x) \quad \text{[S1.37]}$$

And similar to Eqn. [S1.8], we define the production flux by tissue i is

$$F_i = Q_i \cdot C_{new,i}^U(x = l) \quad \text{[S1.38]}$$

where l is the length of the tissue.
Importantly, since the unlabeled old metabolite undergoes identical kinetics as the labeled metabolite, or $C_{old,i}^U(x) = \alpha \cdot C_i^L(x)$, Eqn. [S1.37] becomes

$$C_i(x) = C_i^L(x) + \alpha \cdot C_i^L(x) + C_{new,i}^U(x) \quad \text{[S1.39]}$$

Applying the equation to the arterial and venous sides of the tissue, we get

$$C_i(x = 0) = C_i^L(x = 0) + \alpha \cdot C_i^L(x = 0) \quad \text{[S1.40]}$$

and

$$C_i(x = l) = C_i^L(x = l) + \alpha \cdot C_i^L(x = l) + C_{new,i}^U(x = l) \quad \text{[S1.41]}$$

Rearranging [S1.41],

$$C_{new,i}^U(x = l) = C_i(x = l) \cdot \left(1 - \frac{L_i(x=l)}{L_i(x=0)}\right) \quad \text{[S1.42]}$$

where we have used $L_i(x) = \frac{C_i^L(x)}{C_i(x)}$ and $L_i(0) = \frac{1}{1+\alpha}$ from Eqn. [S1.40].

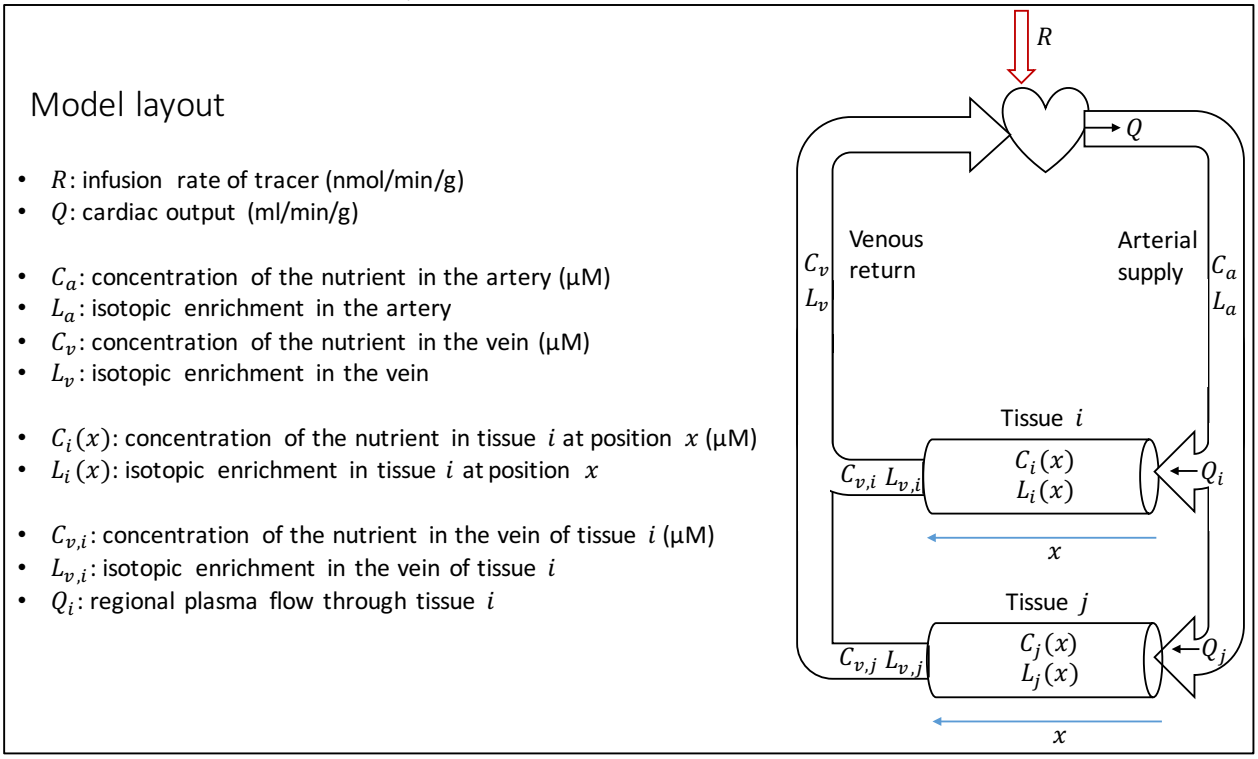

Figure S3. Model layout of the generalized model.

With some parameters defined in Fig. S3, i.e., $C_{v,i} = C_i(x = l)$, $L_{v,i} = L_i(x = l)$, and $L_a = L_i(x = 0)$, Eqn. [S1.42] can be rewritten as

$$C_{new,i}^U(x = l) = C_{v,i} \cdot (1 - \frac{L_{v,i}}{L_a}) \quad [S1.43]$$

Combining Eqns. [S1.38] and [S1.43], we have the tissue-specific production flux

$$F_i = Q_i \cdot C_{v,i} \cdot (1 - \frac{L_{v,i}}{L_a}) \quad [S1.44]$$

where Q_i is the regional plasma flow through the tissue, and $C_{v,i}$ and $L_{v,i}$ are respectively concentration and labeling fraction of the metabolite in the tissue-specific vein.

Note that net uptake of a metabolite by a tissue is given by

$$F_{net,i} = Q_i \cdot (C_{v,i} - C_a) \quad [S1.45]$$

With the production flux and the net flux known, the tissue-specific consumption flux can then be obtained from Eqns. [S1.44]-[S1.45] as

$$F_{consumption,i} = F_i - F_{net,i} = Q_i \cdot C_a \cdot (1 - \frac{C_{v,i}}{C_a} \cdot \frac{L_{v,i}}{L_a}) \quad [S1.46]$$

Turnover flux

Since mass balance in the vein requires that

$$\sum_i Q_i \cdot C_{v,i} = Q \cdot C_v \quad [S1.47]$$

and

$$\sum_i Q_i \cdot C_{v,i} \cdot L_{v,i} = Q \cdot C_v \cdot L_v \quad [S1.48]$$

we get back Eqn. [S1.22], originally derived for a single tissue, now more generally for any number of tissues, using Eqn. [S1.44]

$$F_{circ} = \sum_i F_i = Q \cdot C_v \cdot \frac{L_a - L_v}{L_a} \quad \text{[S1.49]}$$

Finally, using the same derivation procedure as in Eqns. [S1.22]-[S1.24], we again reach the Eqn. [S1.25] for calculating the turnover flux from an isotope infusion experiment.

Note that summing the tissue-specific consumption flux gives

$$\sum_i F_{consumption,i} = F_{circ} + R \quad \text{[S1.50]}$$

Thus, main text Eqn. [2] holds for any number of distinct organs, irrespective of arterial-venous labeling differences.

Supplementary Note 2: Dependence of lactate turnover flux on pyruvate-lactate exchange

The high circulatory turnover flux of lactate (F_{circ}) is sometimes dismissed as an artifact resulting merely from rapid interconversion of pyruvate and lactate[18-22]. Here we quantitatively assess the requirements for obtaining the high observed F_{circ} for lactate. For simplicity, we consider only two metabolite pools, *tissue pyruvate* and *circulating lactate* (Fig. S4). There is bidirectional flux between them, represented by J_f and J_r. Importantly, unlike scrambling of pyruvate and lactate within the cell, interconversion of tissue pyruvate and circulating lactate has the physiological function of uncoupling, at the cellular level, glycolysis from lactate/pyruvate metabolism.

In addition, to Jf and Jr, pyruvate is produced by glycolysis (potentially additional pathways such as amino acid catabolism) via flux J_g and consumed by the TCA cycle via flux J_t. *R* is the infusion rate of isotopic-labeled lactate. Initially, we do not consider gluconeogenesis; then, we show that including gluconeogenesis does not change impact the conclusions.

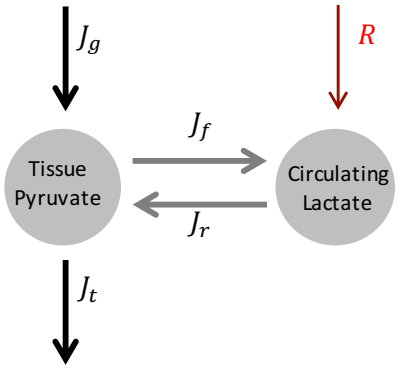

Figure S4. Flux model for evaluating the factors impacting measurement of F_{circ} for lactate.

At steady state, the pool sizes of both metabolites remain unchanged. By mass balance,

$$J_g + J_r = J_f + J_t \quad \text{[S2.1]}$$

and

$$R + J_f = J_r \quad \text{[S2.2]}$$

The labeled fractions of both pools are also constant at steady state. Where L_l and P_l are the labeled fractions of lactate and pyruvate, isotope balancing (under the assumption that glycolysis produces only unlabeled pyruvate) yields

$$L_l J_r = P_l\left(J_f + J_t\right) \quad \text{[S2.3]}$$

and

$$R + P_l J_f = L_l J_r \quad \text{[S2.4]}$$

Solving for P_l and L_l from Eqns. [S1.2]-[S1.4], we get

$$P_l = \frac{R}{J_t} \quad \text{[S2.5]}$$

and

$$L_l = \frac{1+\frac{J_f}{J_t}}{1+\frac{J_f}{R}} \quad [S2.6]$$

Since $J_f \leq J_r$ (according to Eqn. [S2.2]), J_f can be regarded as the exchange flux between tissue pyruvate and circulating lactate, while the flux difference $J_r - J_f$ is the net flux from circulating lactate to tissue pyruvate. For fast exchange flux, $J_f \gg J_t$, it follows that $L_l \to P_l = \frac{R}{J_t}$. And for slow exchanging flux, i.e., $J_f \to 0$, we have $L_l \to 1$.

As the turnover flux F_{circ} of lactate is given by

$$L_l = \frac{R}{R+F_{circ}} \quad [S2.7]$$

combining Eqns. [S2.6] and [S2.7] and utilizing Eqn. [S2.1], we get

$$F_{circ} = J_g \cdot \frac{J_f}{J_t+J_f} \quad [S2.8]$$

which is illustrated in Extended Data Fig. 2a. Thus, F_{circ} is bounded by the whole body rate of tissue pyruvate production from nutrients *other than* lactate: mere exchange between pyruvate and lactate cannot produce large F_{circ}. This is evident in the chemistry of the process, as, in the absence of additional reactions, pyruvate-lactate exchange does not change the lactate labeling pattern. At the same time, to obtain large F_{circ} approaching the upper bound, it is necessary for exchange between circulating lactate and tissue pyruvate to be rapid, i.e. faster than the rate of pyruvate production from nutrients other than lactate, such that most tissue pyruvate become circulating lactate (and conversely most tissue pyruvate comes from circulating lactate). Thus, large F_{circ} for lactate implies that most tissue pyruvate comes from circulating lactate (rather than directly from glucose), and thus that glucose feeds the TCA cycle via circulating lactate.

The rapid exchange between circulating lactate and tissue pyruvate requires high lactate dehydrogenase (LDHA/B) activity and fast lactate transport across the plasma membrane through monocarboxylate transporters (MCT1-4). It is possible that the rapid exchange is facilitated by channeling mediated by co-localization of pyruvate kinase, LDH, and/or MCT or that circulating lactate is channeled into the TCA cycle by molecular complex involving an MCT, LDH, and the mitochondrial pyruvate carrier MPC[23,24], although we do not invoke such channeling to explain our observations.

Finally, to demonstrate that including gluconeogenesis does not change our conclusion, consider a model including also gluconeogenesis flux J_{gluc} from pyruvate to glucose (Fig. S5), in addition to the glycolytic flux J_{glyc} in the opposite direction. Similar to the simpler model, we can write down mass balance equations for the total pool of each metabolite,

$$J_g + J_{gluc} = J_{glyc} \quad [S2.9]$$

$$J_{glyc} + J_r = J_{gluc} + J_f + J_t \quad [S2.10]$$

and

$$R + J_f = J_r \quad [S2.11]$$

Note that Eqn. [S2.11] is identical to Eqn. [S2.2], as the reactions for circulating lactate are the same in the two models, and combining Eqns. [S2.9-10] yields

$$J_g + J_r = J_f + J_t \quad [S2.12]$$

which simply recovers Eqn. [S2.1].

For the labeled pool of each metabolite, we can write the mass balance equation,

$$G_l \cdot J_{glyc} = P_l \cdot J_{gluc} \quad [S2.13]$$

$$L_l \cdot J_r + G_l \cdot J_{glyc} = P_l \cdot (J_{gluc} + J_f + J_t) \quad [S2.14]$$

and

$$R + P_l \cdot J_f = L_l \cdot J_r \quad [S2.15]$$

Eqn. [S2.15] is Eqn. [S2.4], and Eqn. [S2.3] can be recovered by combining Eqns.[S2.13-14].

We have shown that Eqns. [S2.1-4] are valid here in this more complicated model. As Eqns. [S2.1-4] are sufficient to derive Eqn. [S2.8], this equation and thus all of the conclusions apply also in the presence of gluconeogenesis.

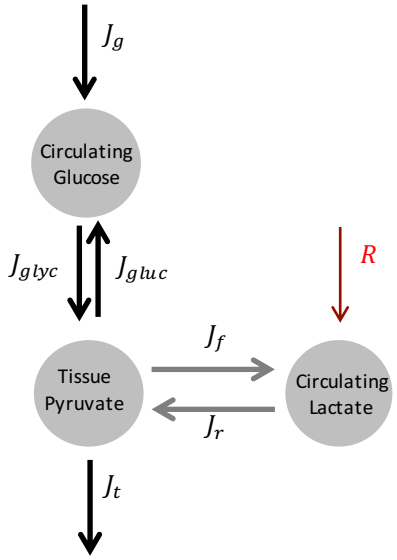

Figure S5. A more complicated flux model for evaluating the factors impacting measurement of F_{circ} for lactate.

Supplementary Note 3: Determination of direct circulating nutrient contributions to individual tissues' TCA

Here we describe how to calculate quantitatively the direct contributions to a tissue's TCA cycle by different circulating nutrients. By direct, we refer to the circulating nutrient being converted into TCA metabolites within the tissue, without passing through the circulation as some other metabolite. Based on our available tissue TCA labeling data, we consider glucose, lactate, and glutamine as circulating TCA substrates. In essence, this model determines the quantitative TCA contributions of circulating glucose, glutamine, and lactate based on data from infusing each in labeled form, taking into account the extent to which labeled infusion of any one also labels the others. Note that this accounting for transfer of label from infused tracer to other circulating metabolites is essential for accurate understanding of tissue substrate usage.

Fig. S6 shows four relevant direct fluxes feeding the TCA, J_{glc} from circulating glucose, J_{lac} from circulating lactate, J_{gln} from circulating glutamine, and J_{other} from all other sources. The three key nutrients may interconvert (e.g. via glycolysis and gluconeogenesis), but for simplicity we assume that they do not interconvert with other nutrients. The sum of the incoming fluxes is equal to the TCA flux J_{TCA}, i.e.,

$$J_{glc} + J_{lac} + J_{gln} + J_{other} = J_{TCA}. \quad [S3.1]$$

Here, all fluxes are in units of per carbon atom and J_{TCA} reflects the flux of all carbon atoms entering the TCA cycle (i.e. sum of anaplerosis and TCA turning) or equivalently leaving the TCA (by mass balance).

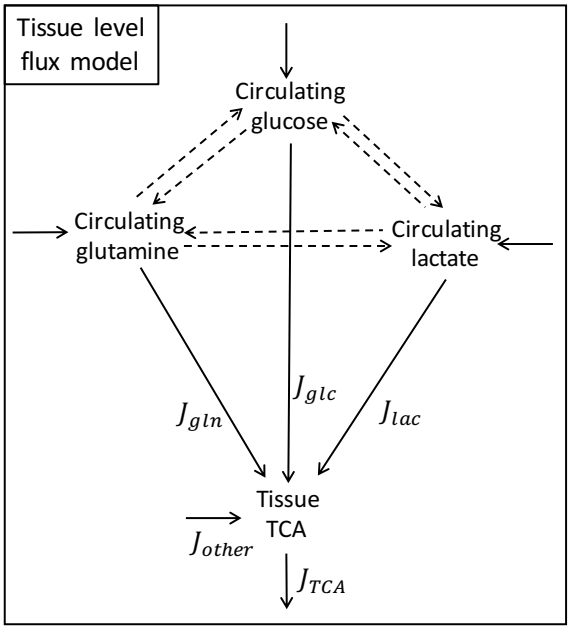

Figure S6. Schematic of model for calculating tissue-specific metabolism of glucose, lactate, and glutamine. For visual clarity, the reactions interconverting the three circulating nutrients are shown as dashed lines.

With the infusion of any of the three ^{13}C tracers, mass balance of labeled form of metabolites require that

$$L_{glc} \cdot J_{glc} + L_{lac} \cdot J_{lac} + L_{gln} \cdot J_{gln} = L_{TCA} \cdot J_{TCA} \quad [S3.2]$$

where L_{glc}, L_{lac}, L_{gln}, and L_{TCA} are the labeled fraction of circulating glucose, circulating lactate, circulating glutamine, and TCA intermediates, respectively.
Dividing both sides of Eqn. [2] by J_{TCA}, we have

$$L_{glc} \cdot f_{TCA \leftarrow glc} + L_{lac} \cdot f_{TCA \leftarrow lac} + L_{gln} \cdot f_{TCA \leftarrow gln} = L_{TCA} \quad [S3.3]$$

where $f_{TCA \leftarrow glc} = \frac{J_{glc}}{J_{TCA}}$, $f_{TCA \leftarrow lac} = \frac{J_{lac}}{J_{TCA}}$, and $f_{TCA \leftarrow gln} = \frac{J_{gln}}{J_{TCA}}$, being the fractional TCA contribution by circulating glucose, circulating lactate, and circulating glutamine, respectively.

For convenience, we normalize the metabolite labeling with the labeling of infused metabolite in serum. For ^{13}C-glucose infusion, after dividing both sides by L_{glc}, Eqn. [S3.3] becomes

$$f_{TCA \leftarrow glc} + f_{TCA \leftarrow lac} \cdot L_{lac \leftarrow glc} + f_{TCA \leftarrow gln} \cdot L_{gln \leftarrow glc} = L_{TCA \leftarrow glc} \quad [S3.4]$$

where $L_{lac \leftarrow glc} = \frac{L_{lac}}{L_{glc}}$, $L_{gln \leftarrow glc} = \frac{L_{gln}}{L_{glc}}$, and $L_{TCA \leftarrow glc} = \frac{L_{TCA}}{L_{glc}}$.

Similarly, for ^{13}C-lactate infusion and ^{13}C-glutamine infusion, we have respectively

$$f_{TCA \leftarrow glc} \cdot L_{glc \leftarrow Lac} + f_{TCA \leftarrow lac} + f_{TCA \leftarrow gln} \cdot L_{gln \leftarrow lac} = L_{TCA \leftarrow lac} \quad [S3.5]$$

and

$$f_{TCA \leftarrow glc} \cdot L_{glc \leftarrow gln} + f_{TCA \leftarrow lac} \cdot L_{lac \leftarrow gln} + f_{TCA \leftarrow gln} = L_{TCA \leftarrow gln} \quad [S3.6]$$

For simpler representation, Eqns. [S3.4-6] can be written in matrix format,

$$\begin{pmatrix} 1 & L_{lac \leftarrow glc} & L_{gln \leftarrow glc} \\ L_{glc \leftarrow lac} & 1 & L_{gln \leftarrow lac} \\ L_{glc \leftarrow gln} & L_{lac \leftarrow gln} & 1 \end{pmatrix} \begin{pmatrix} f_{TCA \leftarrow glc} \\ f_{TCA \leftarrow lac} \\ f_{TCA \leftarrow gln} \end{pmatrix} = \begin{pmatrix} L_{TCA \leftarrow glc} \\ L_{TCA \leftarrow lac} \\ L_{TCA \leftarrow gln} \end{pmatrix} \quad [S3.7]$$

The 3x3 matrix describes the degree of inter-conversion between the three circulating nutrients. The labeling of the TCA cycle is the result of direct contributions transformed by this matrix. The matrix is the same for all tissues while the TCA labeling vector is unique to each tissue. Note also that this formulation can be generalized to any number of circulating nutrients. While this approach is an advance over prior methods that did not distinguish direct versus indirect contributions (e.g. glucose feeding the TCA cycle via circulating lactate), it only corrects for indirect contributions of circulating metabolites in the matrix (e.g. if glucose feeds the TCA via serine, because serine is not included in the matrix, glucose's contribution via serine will be mistakenly counted as a direct glucose contribution). It is important to apply this approach (eventually expanded to include most major circulating nutrients) to properly understand tissue and tumor fuel selection.

Since all the L's (labeled fraction) are known, the vector of f's can be solved. Applying Eqn. [S3.7] to each of the studied tissues in fasting mice, we get the fractional TCA contributions by circulating glucose, lactate, and glutamine for each tissue (Table S1).

	Succinate			Malate			Average		
	$f_{TCA\leftarrow glc}$	$f_{TCA\leftarrow lac}$	$f_{TCA\leftarrow gln}$	$f_{TCA\leftarrow glc}$	$f_{TCA\leftarrow lac}$	$f_{TCA\leftarrow gln}$	$f_{TCA\leftarrow glc}$	$f_{TCA\leftarrow lac}$	$f_{TCA\leftarrow gln}$
Brain	0.65±0.02	0.17±0.03	0.02±0.01	0.66±0.02	0.16±0.03	0.02±0.01	0.66±0.03	0.17±0.04	0.02±0.01
Muscle	0.08±0.05	0.21±0.03	0.07±0.01	0.05±0.04	0.23±0.03	0.07±0.01	0.07±0.06	0.22±0.04	0.07±0.02
Kidney	-0.06±0.05	0.37±0.04	0.14±0.01	-0.04±0.04	0.35±0.04	0.12±0.00	-0.05±0.06	0.36±0.05	0.13±0.01
Liver	-0.04±0.02	0.29±0.02	0.16±0.01	-0.03±0.02	0.28±0.03	0.13±0.01	-0.03±0.03	0.28±0.04	0.14±0.01
Spleen	-0.00±0.03	0.12±0.03	0.27±0.02	-0.00±0.03	0.13±0.03	0.29±0.03	-0.00±0.04	0.13±0.04	0.28±0.04
Pancreas	-0.00±0.03	0.15±0.03	0.36±0.08	-0.01±0.03	0.18±0.03	0.31±0.07	-0.01±0.04	0.17±0.04	0.33±0.11
Lung	0.01±0.03	0.22±0.02	0.07±0.01	0.01±0.03	0.29±0.02	0.09±0.01	0.01±0.04	0.25±0.03	0.08±0.02
Heart	0.03±0.05	0.21±0.04	0.01±0.00	0.02±0.04	0.21±0.03	0.02±0.00	0.02±0.07	0.21±0.05	0.01±0.01
Adipose	-0.02±0.03	0.23±0.03	0.11±0.01	-0.01±0.03	0.21±0.02	0.13±0.01	-0.01±0.04	0.22±0.03	0.12±0.01
S. Intestine	0.01±0.03	0.11±0.03	0.34±0.02	-0.01±0.03	0.15±0.03	0.29±0.02	0.00±0.04	0.13±0.04	0.31±0.03

Table S1. Fractional TCA contributions by circulating glucose, lactate, and glutamine for each tissue in fasting mice. Values are mean ± SEM. Errors were obtained by error propagation. Values in the "average" columns are shown in Fig. 2e.

Similarly, we calculate the fractional TCA contributions by the three circulating nutrients in the fed mice (Table S2) and in tumors (Table S3).

	Succinate			Malate			Average		
	$f_{TCA\leftarrow glc}$	$f_{TCA\leftarrow lac}$	$f_{TCA\leftarrow gln}$	$f_{TCA\leftarrow glc}$	$f_{TCA\leftarrow lac}$	$f_{TCA\leftarrow gln}$	$f_{TCA\leftarrow glc}$	$f_{TCA\leftarrow lac}$	$f_{TCA\leftarrow gln}$
Brain	0.71±0.03	0.11±0.02	0.01±0.01	0.74±0.03	0.11±0.02	0.02±0.01	0.72±0.04	0.11±0.03	0.01±0.01
Muscle	0.21±0.06	0.24±0.02	0.05±0.01	0.20±0.06	0.24±0.03	0.05±0.01	0.21±0.09	0.24±0.03	0.05±0.01
Kidney	0.08±0.04	0.36±0.04	0.15±0.01	0.07±0.04	0.35±0.03	0.13±0.01	0.07±0.05	0.35±0.05	0.14±0.01
Liver	0.04±0.02	0.25±0.02	0.14±0.01	0.08±0.02	0.22±0.01	0.11±0.01	0.06±0.03	0.23±0.02	0.12±0.02
Spleen	0.01±0.02	0.15±0.03	0.24±0.00	0.04±0.03	0.15±0.03	0.26±0.01	0.02±0.03	0.15±0.04	0.25±0.01
Pancreas	0.04±0.02	0.18±0.02	0.46±0.03	0.01±0.03	0.21±0.02	0.39±0.02	0.02±0.04	0.19±0.03	0.42±0.03
Lung	0.10±0.02	0.20±0.01	0.03±0.01	0.12±0.02	0.27±0.01	0.10±0.01	0.11±0.03	0.23±0.02	0.06±0.01
Heart	0.28±0.07	0.26±0.04	0.01±0.01	0.29±0.05	0.24±0.04	0.02±0.01	0.28±0.09	0.25±0.06	0.01±0.01
Adipose	0.05±0.03	0.23±0.02	0.06±0.03	0.08±0.02	0.18±0.02	0.11±0.00	0.06±0.04	0.20±0.02	0.09±0.03
S. Intestine	-0.02±0.04	0.20±0.04	0.23±0.05	-0.00±0.04	0.20±0.04	0.21±0.05	-0.01±0.05	0.20±0.06	0.22±0.07

Table S2. Fractional TCA contributions by circulating glucose, lactate, and glutamine for each tissue in fed mice. Values are mean ± SEM. Errors were obtained by error propagation. Values in the "average" columns are shown in Fig. 3c.

	Succinate		Malate				Average		
	$f_{TCA\leftarrow glc}$	$f_{TCA\leftarrow lac}$	$f_{TCA\leftarrow gln}$	$f_{TCA\leftarrow glc}$	$f_{TCA\leftarrow lac}$	$f_{TCA\leftarrow gln}$	$f_{TCA\leftarrow glc}$	$f_{TCA\leftarrow lac}$	$f_{TCA\leftarrow gln}$
KP lung	0.03±0.04	0.27±0.04	0.11±0.03	0.04±0.03	0.29±0.03	0.12±0.01	0.04±0.05	0.28±0.05	0.12±0.03
KL lung	0.05±0.04	0.29±0.06	0.14±0.05	0.08±0.03	0.28±0.06	0.16±0.03	0.07±0.05	0.28±0.09	0.15±0.06
KPC	-0.03±0.04	0.16±0.04	0.27±0.02	-0.02±0.05	0.16±0.06	0.24±0.02	-0.02±0.07	0.16±0.07	0.25±0.03

Table S3. Fractional TCA contributions by circulating glucose, lactate, and glutamine for each of the three tumors. Values are mean ± SEM. Errors were obtained by error propagation. Values in the "average" columns are shown in Fig. 4d.

Supplementary Note 4: Glucose and lactate fluxes measured by plasma metabolite labeling

Steady-state labeling of circulating glucose and lactate can be used to determine the whole body fluxes of glucose and lactate shown in Fig. S7: glucose and lactate are interconverted via the fluxes J_2 and J_3; glucose and lactate feed directly to tissue TCA via fluxes J_6 and J_5; and both glucose and lactate are produced from other substrates (in unlabeled form) via fluxes J_1 and J_4.

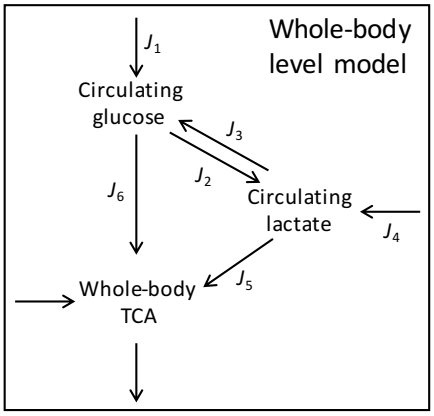

Figure S7. Layout of the whole-body flux model.

In this simple model, all fluxes are in units of nmol C/min/g. For example, to convert into units of nmol glucose/min/g, divide J_1 by 6. By defining fluxes on a per carbon atom basis, there is no need to account for the 2:1 stoichiometry between lactate and glucose.

Mass balance of the glucose and lactate leads to the following two equations,

$$J_1 + J_3 = J_2 + J_6 \quad [S4.1]$$

and

$$J_2 + J_4 = J_3 + J_5 \quad [S4.2]$$

Next, we introduce the turnover flux on an average per carbon atom basis for glucose and lactate as F'_{glc} and F'_{lac}, respectively. These average-atom turnover fluxes (F') differ from F_{circ} in two respects: (i) scaling for the number of carbon atoms in the molecule and (ii) rather than treating any biochemical transformation which alters the labeling pattern of the infused metabolite as equivalent (as is done for F_{circ}), instead accounting for the extent to which average carbon atom labeling is altered by the transformation. Thus, while both F' and F_{circ} are calculated based on Eqn. [2], F' Is calculated based on average carbon atom labeling as defined in Eqn. [S1.36]. The average-atom turnover fluxes can be expressed in terms of the fluxes illustrated in Fig. S6,

$$J_1 \cdot \frac{J_2}{J_2+J_6} + J_4 = F'_{lac} \quad [S4.3]$$

and

$$J_4 \cdot \frac{J_3}{J_3+J_5} + J_1 = F'_{glc} \quad [S4.4]$$

Finally, under ^{13}C-glucose infusion, the labeled fraction of lactate ($f_{lac\leftarrow glc}$) can be expressed as

$$\frac{J_2}{J_2+J_4} = f_{lac\leftarrow glc} \quad [S4.5]$$

and under ^{13}C-lactate infusion, the labeled fraction of glucose ($f_{glc\leftarrow lac}$) can be similarly expressed as

$$\frac{J_3}{J_1+J_3} = f_{glc\leftarrow lac} \quad [S4.6]$$

Since F'_{lac}, F'_{glc}, $f_{lac\leftarrow glc}$, and $f_{glc\leftarrow lac}$ have been measured and thus are known parameters (Table S4), Eqns. [S4.1]-[S4.6] can be solved algebraically (without any fitting) to obtain the expressions of the six fluxes,

$$J_1 = \frac{F'_{glc}\cdot(1-f_{glc\leftarrow lac})}{1-f_{glc\leftarrow glc}\cdot f_{glc\leftarrow lac}} \quad [S4.7]$$

$$J_2 = \frac{F'_{lac}\cdot f_{lac\leftarrow glc}}{1-f_{lac\leftarrow glc}\cdot f_{glc\leftarrow lac}} \quad [S4.8]$$

$$J_3 = \frac{F'_{glc}\cdot f_{glc\leftarrow lac}}{1-f_{lac\leftarrow glc}\cdot f_{glc\leftarrow lac}} \quad [S4.9]$$

$$J_4 = \frac{F'_{lac}\cdot(1-f_{lac\leftarrow glc})}{1-f_{lac\leftarrow glc}\cdot f_{glc\leftarrow lac}} \quad [S4.10]$$

$$J_5 = \frac{F'_{lac}-F'_{glc}\cdot f_{glc\leftarrow lac}}{1-f_{lac\leftarrow glc}\cdot f_{glc\leftarrow lac}} \quad [S4.11]$$

and

$$J_6 = \frac{F'_{glc}-F'_{lac}\cdot f_{lac\leftarrow glc}}{1-f_{lac\leftarrow glc}\cdot f_{glc\leftarrow lac}} \quad [S4.12]$$

The numerical values of the six fluxes for fasted, fed, and anesthetized states are given in Table S4.

To end, we note that the large whole-body lactate flux requires source(s) for the circulating lactate. In the simplest case, this could be a specific tissue; however, we consider it more likely that lactate production is more broadly distributed throughout the body. Given the rapid exchange between lactate and serum, it is intriguing to speculate that red blood cells might be responsible for a substantial fraction of the observed production of circulating lactate. This is consistent with red blood cells relying sole on glycolysis for energy. The magnitude of the whole body lactate production that we observed, however, is far beyond that expected based on prior literature regarding erythrocyte metabolism. Specifically, erythrocyte lactate production has been measured, with the maximal lactate production rate measured in the reference[25] equal to 3.5 µmol per hr per ml of packed red blood cells. Assuming that the blood content of mouse is 0.07 ml/g[26] and 40% of blood cell volume is erythrocytes, we get that the lactate production flux by erythrocytes is 3.5 µmol/hr/min x 0.07 ml/g x 0.4 = 1.6 nmol/min/g, which is less than 0.5% of the lactate turnover flux in fasted state. It is possible that *in vitro* measurements dramatically underestimate the *in vivo* metabolic activity of erythrocytes. More likely, other tissue compartments or cell types, yet to be determined, play a central role in circulating lactate production.

	Measured quantities		Calculated quantities		
Physiological state	Quantity	Value	Quantity	Value (nmol C/min/g)	Shown in figure
Fasted	F'_{lac}	886±104 nmol C/min/g	J_1	652±81	Fig. 2f
	F'_{glc}	770±92 nmol C/min/g	J_2	740±95	
	$f_{lac\leftarrow glc}$	0.65±0.02	J_3	336±69	
	$f_{glc\leftarrow lac}$	0.34±0.04	J_4	398±52	
			J_5	802±140	
			J_6	249±149	
Fed	F'_{lac}	1318±160 nmol C/min/g	J_1	2480±276	Fig. 3d
	F'_{glc}	2573±285 nmol C/min/g	J_2	1138±148	
	$f_{lac\leftarrow glc}$	0.77±0.03	J_3	404±68	
	$f_{glc\leftarrow lac}$	0.14±0.02	J_4	340±60	
			J_5	1074±188	
			J_6	1746±351	
Anesthetized	F'_{lac}	341±36 nmol C/min/g	J_1	257±31	Extended Data Fig. 7
	F'_{glc}	271±33 nmol C/min/g	J_2	348±42	
	$f_{lac\leftarrow glc}$	0.82±0.01	J_3	81±23	
	$f_{glc\leftarrow lac}$	0.24±0.03	J_4	76±10	
			J_5	343±47	
			J_6	-10±56	

Table S4. Experimentally measured and calculated fluxes, for the fasted, fed, and anesthetized mice. All values are means ± SEM. For measured fluxes, errors were determined by combining standard errors of biological replicates and 10% inherent error of the infusion method. For calculated fluxes, errors were determined by error propagation based on errors in the measured values.

Supplementary Tables

Supplementary Table 1: Infusion parameters for tracers used in this study.

Nutrient	Tracer used	Tracer concentration (mM)	Infusion rate (µl/min/g)	Labeling of tracer in serum
Lactate	[U-13C]sodium lactate	5% w/w	0.1	0.109
Glucose	[U-13C]glucose	200	0.1	0.117
Acetate	[U-13C]sodium acetate	50	0.05	0.033
Alanine	[U-13C]alanine	200	0.05	0.125
Pyruvate	[U-13C]pyruvate	400	0.1	0.098
Glycerol	[U-13C]glycerol	100	0.1	0.158
Glutamine	[U-13C]glutamine	100	0.1	0.180
3-Hydroxybutyrate	[U-13C]sodium 3-hydroxybutyrate	50	0.05	0.055
Palmitic acid	[U-13C]sodium palmitate	1.85	0.2	0.015
Glycine	[U-13C]glycine	20	0.1	0.084
Taurine	[U-13C]taurine	10	0.1	0.049
Serine	[U-13C]serine	20	0.1	0.094
Citrate	[2,4-13C]citric acid	10	0.1	0.058
Leucine	[U-13C; 15N]leucine	15.6	0.1	0.119
Valine	[U-13C; 15N]valine	10	0.1	0.094
Lysine	[U-13C; U-15N]lysine:2HCl	11.6	0.1	0.111
Arginine	[U-13C; U-15N]arginine:HCl	35	0.1	0.280
Tyrosine	[U-13C; 15N]tyrosine	3	0.1	0.036
Threonine	[U-13C; 15N]threonine	7.7	0.1	0.092
Proline	[U-13C]proline	10	0.1	0.120
Isoleucine	[U-13C; 15N]isoleucine	9.7	0.1	0.130
Asparagine	[U-13C]asparagine	10	0.1	0.133
Phenylalanine	[U-13C; 15N]phenylalanine	9	0.1	0.132
2-Oxoglutarate	[U-13C]2-oxoglutarate disodium	5	0.1	0.079
Histidine	[U-13C; U-15N]histidine:HCl	5	0.1	0.091
Methionine	[U-13C; 15N]methionine	7	0.1	0.152
Succinate	[U-13C]succinic acid	10	0.05	0.139
Creatine	[Guanidino-13C]creatine	10	0.1	0.278
Tryptophan	[U-13C; U-15N]tryptophan	2.6	0.1	0.102
Malate	[U-13C]malic acid	10	0.05	0.200
Betaine	[D11]betaine	1	0.1	0.059

References

1 Wolfe, R. R. & Chinkes, D. L. *Isotope tracers in metabolic research: principles and practice of kinetic analysis*. (John Wiley & Sons, 2005).

2 Tserng, K. & Kalhan, S. C. Calculation of substrate turnover rate in stable isotope tracer studies. *American Journal of Physiology-Endocrinology And Metabolism* **245**, E308-E311 (1983).

3 Wootton, R., Ford, G., Cheng, K. & Halliday, D. Calculation of turnover rates in stable-isotope studies. *Physics in medicine and biology* **30**, 1143 (1985).

4 McCabe, B. J. & Previs, S. F. Using isotope tracers to study metabolism: application in mouse models. *Metabolic Engineering* **6**, 25-35, doi:http://dx.doi.org/10.1016/j.ymben.2003.09.003 (2004).

5 Katz, J., Okajima, F., Chenoweth, M. & Dunn, A. The determination of lactate turnover in vivo with 3H-and 14C-labelled lactate. The significance of sites of tracer administration and sampling. *Biochemical Journal* **194**, 513-524 (1981).

6 Layman, D. K. & Wolfe, R. R. Sample site selection for tracer studies applying a unidirectional circulatory approach. *American Journal of Physiology-Endocrinology and Metabolism* **253**, E173-E178 (1987).

7 Katz, J. & Wolfe, R. R. On the measurement of lactate turnover in humans. *Metabolism* **37**, 1078-1080 (1988).

8 Binder, N. D., Day, D., Battaglia, F. C., Meschia, G. & Sparks, J. W. Role of the circulation in measurement of lactate turnover rate. *Journal of Applied Physiology* **70**, 1469-1476 (1991).

9 Norwich, K. H. Sites of infusion and sampling for measurement of rates of production in steady state. *American Journal of Physiology-Endocrinology and Metabolism* **263**, E817-E822 (1992).

10 Sacca, L., Toffolo, G. & Cobelli, C. VA and AV modes in whole body and regional kinetics: domain of validity from a physiological model. *American Journal of Physiology-Endocrinology and Metabolism* **263**, E597-E606 (1992).

11 Meschia, G. On the measurement of turnover in vivo. *American Journal of Physiology-Endocrinology and Metabolism* **265**, E348-E349 (1993).

12 Gjedde, S. B. & Gjeode, A. Organ blood flow rates and cardiac output of the BALB/c mouse. *Comparative Biochemistry and Physiology Part A: Physiology* **67**, 671-674 (1980).

13 Medinsky, M. A., Leavens, T. L., Csanády, G. A., Gargas, M. L. & Bond, J. A. In vivo metabolism of butadiene by mice and rats: a comparison of physiological model predictions and experimental data. *Carcinogenesis* **15**, 1329-1340 (1994).

14 Barbee, R. W., Perry, B. D., Re, R. N. & Murgo, J. P. Microsphere and dilution techniques for the determination of blood flows and volumes in conscious mice. *American Journal of Physiology-Regulatory, Integrative and Comparative Physiology* **263**, R728-R733 (1992).

15 Davies, B. & Morris, T. Physiological parameters in laboratory animals and humans. *Pharmaceutical research* **10**, 1093-1095 (1993).

16 Janssen, B., Debets, J., Leenders, P. & Smits, J. Chronic measurement of cardiac output in conscious mice. *American Journal of Physiology-Regulatory, Integrative and Comparative Physiology* **282**, R928-R935 (2002).
17 Sugimoto, M. *et al.* MMMDB: Mouse multiple tissue metabolome database. *Nucleic acids research* **40**, D809-D814 (2012).
18 Wolfe, R. R. Isotopic measurement of glucose and lactate kinetics. *Annals of medicine* **22**, 163-170 (1990).
19 Wolfe, R. R., Jahoor, F. & Miyoshi, H. Evaluation of the isotopic equilibration between lactate and pyruvate. *American Journal of Physiology-Endocrinology And Metabolism* **254**, E532-E535 (1988).
20 Zhang, X.-j., Baba, H. & Wolfe, R. R. Further evaluation of isotopic equilibration between labeled pyruvate and lactate. *The Journal of Nutritional Biochemistry* **4**, 218-221 (1993).
21 Romijn, J., Chinkes, D., Schwarz, J. & Wolfe, R. Lactate-pyruvate interconversion in blood: implications for in vivo tracer studies. *American Journal of Physiology-Endocrinology And Metabolism* **266**, E334-E340 (1994).
22 Sahlin, K. Lactate production cannot be measured with tracer techniques. *American Journal of Physiology-Endocrinology And Metabolism* **252**, E439-E440 (1987).
23 Herzig, S. *et al.* Identification and functional expression of the mitochondrial pyruvate carrier. *Science* **337**, 93-96 (2012).
24 Bricker, D. K. *et al.* A mitochondrial pyruvate carrier required for pyruvate uptake in yeast, Drosophila, and humans. *Science* **337**, 96-100, doi:10.1126/science.1218099 (2012).
25 Rose, I. A. & Warms, J. V. Control of glycolysis in the human red blood cell. *Journal of Biological Chemistry* **241**, 4848-4854 (1966).
26 Parasuraman, S., Raveendran, R. & Kesavan, R. Blood sample collection in small laboratory animals. *Journal of Pharmacology and Pharmacotherapeutics* **1**, 87 (2010).